Three-dimensional superconducting behavior and thermodynamic parameters of $HgBa_2Ca_{0.86}Sr_{0.14}Cu_2O_{6-\delta}$

Mun-Seog Kim
Department of Physics, Pohang University of Science and Technology, Pohang 790-784, South Korea
and Department of Physics, Chungbuk National University, Cheongju 360-763, South Korea

Sung-Ik Lee
Department of Physics, Pohang University of Science and Technology, Pohang 790-784, South Korea

Seong-Cho Yu
Department of Physics, Chungbuk National University, Cheongju 360-763, South Korea

Nam H. Hur
Korea Research Institute of Standards and Science, Taedok Science Town, Taejon 305-600, South Korea

(Received 7 November 1995)

This study measures the temperature dependence of reversible magnetization of grain-aligned $HgBa_2Ca_{0.86}Sr_{0.14}Cu_2O_{6-\delta}$ high-T_c superconductor with external magnetic fields parallel to the c axis. The magnetization is field independent at $T^* = 114.5$ K, which indicates strong thermal vortex fluctuations. From the vortex fluctuation model, the lower limit of coherence length along the c axis $\xi_c(0) \simeq 2$ and the anisotropy ratio $\gamma \leqslant 7.7$ has been obtained, which implies that this sample is anisotropic three-dimensional (3D) superconductor as $Y_1Ba_2Cu_3O_{7-\delta}$. These results are supported by good 3D scaling behavior of high-field magnetization around $T_c(H)$ as a function of $[T-T_c(H)]/(TH)^{2/3}$. The thermodynamic critical field $H_c(T)$ and the Ginzburg-Landau parameter $\kappa = 114.8$ were extracted from the model of Hao *et al.* Also, the various thermodynamic parameters were obtained: the penetration depth $\lambda_{ab}(0) = 1913$ Å, coherence length $\xi_{ab}(0) = 13.9$ Å, and the zero temperature upper critical field $H_{c2}(0) = 170.4$ T.

I. INTRODUCTION

One of the intriguing features of Josephson coupled layered superconductors is the existence of the field independent magnetization point. This peculiar behavior could be explained by the vortex fluctuation effect, i.e., the entropy contribution to the free energy due to thermal distortions of two-dimensional (2D) vortex pancakes, suggested by Bulaevskii, Ledvij, and Kogan (BLK model).[1] This effect plays an important role in the thermodynamic properties for highly anisotropic superconductors. For example, in $Bi_2Sr_2CaCu_2O_{8-\delta}$ (Bi-2212), the magnetization significantly deviates from the prediction of the mean-field theory.[2] Moreover, the Ginzburg-Landau parameter $\kappa(T)$ and upper critical field $H_{c2}(T)$ derived from that magnetization data show unphysical increase with increasing temperature for a broad temperature range below T_c. The field independent magnetization point has been also observed in three-dimensional (3D) superconductors such as $YBa_2Cu_3O_{7-\delta}$ (Y-123) (Ref. 3) and $YBa_2Cu_4O_8$ (Y-124).[4] But, in these superconductors, the vortex fluctuation effect is not well investigated quantitatively. This should be studied in detail. The study of these effects is important for the understanding of the nature of the layered superconductors.

This paper reports the experimental results on reversible magnetization for grain aligned $HgBa_2Ca_{0.86}Sr_{0.14}Cu_2O_{6-\delta}$ (Hg-1212). Field-induced magnetic fluctuations are clearly observed near $T_c(H)$, and a crossover of magnetization curves $M(T)$ for various magnetic fields was found at $T^* = 114.5$ K, which indicates the vortex fluctuation effect.

As a member of the Hg-based superconductors, the structure of a Hg-1212 is typical 1212 type structure as Y-123. The main difference between Hg-1212 and Y-123 is the oxygen contents in the rocksalt layers. While the copper perovskitelike blocks of two CuO_2 planes in Y-123 are separated by a plane consisting of CuO chains, the blocks are separated by HgO layers without chain in Hg-1212. The spacing s between two blocks is about 12.7 Å which is between $s \simeq 11.7$ Å for Y-123 (anisotropic 3D) and $s \simeq 15$ Å for Bi-2212 (quasi-2D). Therefore, it is quite interesting to investigate the dimensionality of this superconductor. With this aim, the magnetization data near $T_c(H)$ were analyzed by the BLK model and the high-field scaling law.[5] The model of Hao *et al.*[6,7] was also applied to obtain the various superconducting parameters such as critical fields $H_c(0)$, $H_{c1}(0)$, $H_{c2}(0)$, penetration depth $\lambda(0)$, coherence length $\xi(0)$, and $\kappa(T)$. These values are consistent with the results from scaling analysis. All three analyses, BLK, Hao and Clem's model, and high field scaling law support the conclusion that Hg-1212 is an anisotropic three-dimensional superconductor.

II. EXPERIMENTS

Details on the preparations of $HgBa_2Ca_{0.86}Sr_{0.14}Cu_2O_{6-\delta}$ are given elsewhere.[8,9] The introduction of Sr into the Ca site might increase the stability of the Hg-1212 structure, as observed in the infinite layered compound. The precursors of

0163-1829/96/53(14)/9460(6)/$10.00

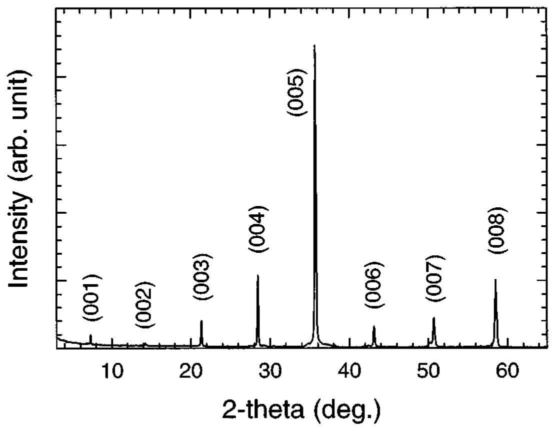

FIG. 1. x-ray-diffraction pattern of c-axis grain aligned $HgBa_2Ca_{0.86}Sr_{0.14}Cu_2O_{6-\delta}$.

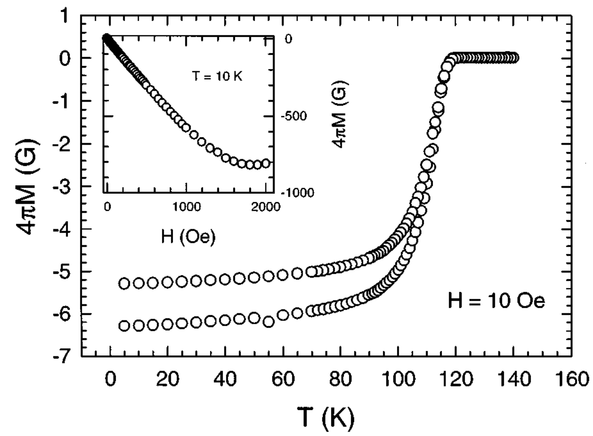

FIG. 2. Temperature dependence of field-cooled and zero-field-cooled magnetization $4\pi M(T)$ for $H = 10$ Oe parallel to c axis. Inset: magnetization versus magnetic field at $T = 10$ K. The slope $-d4\pi M/dH = 0.62$ is estimated by a least-squares fit to low field data.

Ba_2CuO_{3+x} and $Ca_{1-x}Sr_xCuO_2$ were mixed with HgO and compacted into pellets. The pellets were placed inside an alumina tube to avoid the direct contact with a silica tube, and then sealed under vacuum. All the above operations were done in the argon-filled dry box. The sample was heated slowly to 860 °C for 8 h, then sintered at same temperature for 10 h, and then slowly cooled down to room temperature for 10 h. The oxygenation was carried out at 350 °C for 8 h in oxygen atmospheres. This compound has a tetragonal symmetry ($p4/mmm$) with lattice parameters of $a = 3.8584$ Å and $c = 12.6646$ Å. The structure of this compound consists of slabs of CuO_5 square pyramids separated by rocksalt HgO_δ and Ca/Sr layers. Four short Cu-O(1) distances in the plane are 1.931 Å, while the fifth O(2) apical oxygen is 2.81 Å above the plane. These results are close to those reported previously for $HgBa_2Ca_1Cu_2O_{6-\delta}$,[10] suggesting that doping the Ca sites with larger Sr atoms does not produce any significant structural change. To obtain c-axis aligned sample, Farrell's method[11] was employed. The powders were aligned in epoxy with an external magnetic field of 7 T. The size of the cylindrical sample is approximately 9.5 mm long and 3 mm in diameter.

The temperature dependence of magnetization was measured by using a superconducting quantum interference device magnetometer (MPMS, Quantum Design). The measurement in zero-field-cooled and field-cooled magnetization at various magnetic fields was repeated. Weak temperature-dependent contributions originated from the epoxy, and the paramagnetic impurities were appropriately subtracted from the observed values by fitting the magnetization curve at the high temperature region of 200 K$\leqslant T \leqslant$250 K by $C/T+\chi_0$.

III. RESULTS AND DISCUSSION

Figure 1 displays the x-ray powder diffraction pattern of the grain-aligned Hg-1212. All the (hkl) reflections have zero h and k values, which indicates c-axis alignment of the grains. The full width at half maximum (FWHM) in the x-ray rocking curve of (005) is about 1°, which means excellent alignment of grains.

Figure 2 shows the temperature dependence of the magnetization for the magnetic field $H = 10$ Oe parallel to the c axis. The superconducting transition temperature is about 116 K. The superconducting volume fraction f_v is estimated to be 0.625 (62.5%) from the shielding effect, which is also confirmed by the initial slope $-d(4\pi M)/dH = 0.62$ in $M(H)$ curve at 10 K as shown in inset of Fig. 2. With this piece of preliminary information, we now proceed to study the various thermodynamic properties.

A. Crossover of magnetization curves

Figure 3 shows temperature dependence of reversible magnetization for various external magnetic fields. The field independent magnetization M^* appears at $T^* = 114.5$ K. The inset of Fig. 3 shows details of $M(T)$ near the crossover temperature. The corrected value of M^* by volume fraction f_v is 0.08 G.

For the layered superconductors with the high anisotropy ratio $\gamma = \xi_{ab}/\xi_c = \sqrt{m_c/m_{ab}}$, vortices could be easily distorted due to the thermal fluctuations. Therefore, this effect should be considered in describing the reversible magnetization properly. If this extra contribution of thermal distortion is included, then

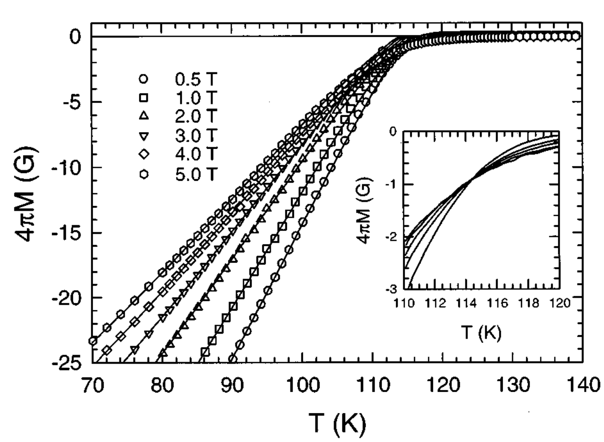

FIG. 3. Temperature dependence of reversible magnetization $4\pi M(T)$ with the theoretical curves (solid line) derived from the model of Hao *et al.* Inset: $4\pi M$ vs T near T^*.

$$-M(T)=\frac{\phi_0}{32\pi^2\lambda_{ab}^2(T)}\ln\frac{\eta H_{c2}}{eH}-\frac{k_BT}{\phi_0 R}\ln\frac{16\pi k_BT\kappa^2}{\alpha\phi_0 RH\sqrt{e}}, \tag{1}$$

where $e = 2.718\ldots$, η and α are constants of order unity, and R is effective interlayer spacing for a quasi-2D system. Even though a superconductor is an anisotropic 3D system, all expressions are retained. But R should be replaced by $C\xi_c(T)$, where C is a numerical factor of the order unity.[1] The first term on the right-hand side denotes reversible magnetization from the London model[12,13] and the second term is originated from this thermal distortion. The slope $\partial M/\partial \ln H$ is

$$\frac{\partial M}{\partial \ln H}=\frac{\phi_0}{32\pi^2\lambda_{ab}^2(T)}[1-g(T)], \tag{2}$$

where

$$g(T)=\frac{32\pi^2k_B}{\phi_0^2R}T\lambda_{ab}^2(T). \tag{3}$$

For large λ and high T, $g(T)$ is important and the magnetization deviates from the standard London behavior of $M\sim\ln H$. In the BLK model, temperature T^* is defined as $g(T^*) = 1$, and the magnetization at this temperature is field independent

$$-M(T^*)\equiv -M^*=\frac{k_BT^*}{R\phi_0}\ln\frac{\eta\alpha}{\sqrt{e}}. \tag{4}$$

In quasi-2D systems, the high-field scaling theory proposed by by Tešanović[14,15] predicts the same relation as Eq. (4) without the ln factor, i.e., $\ln(\eta\alpha/\sqrt{e}) = 1$. Several groups have shown that the R is the same as the distance s between two adjacent CuO_2 blocks for a 2D system such as Bi-2212, $Bi_2Sr_2Ca_2Cu_3O_{10}$ (Bi-2223),[15,16] and PrCeCuO (Ref. 17) compounds. If the relation $\ln(\eta\alpha/\sqrt{e}) = 1$ holds for our case, the estimated R is 68.5 Å. But, comparing with $s\simeq 12.7$ Å obtained from x-ray-diffraction data, this value is too large. This discordance might result from the overestimation of f_v due to the demagnetization effect. But, we expect that uncertainty of f_v is small, because the demagnetization factor of our sample is only about 0.1. The above results lead to the conclusion that the sample is not close to a quasi-2D system at all.

Alternatively, the R could be regarded as $C\xi_c(T)$ assuming an anisotropic 3D system and rewrite Eq. (2) as follows:

$$\frac{\partial M}{\partial \ln H}=\frac{\phi_0}{32\pi^2\lambda_{ab}^2(T)}-\frac{k_BT\gamma\kappa}{\phi_0 C\lambda_{ab}(T)}, \tag{5}$$

using the relation $\xi_c(T)=\lambda_{ab}(T)/\gamma\kappa$. Figure 4 shows the temperature dependence of the slope $\partial M/\partial \ln H$. The solid line represents our attempts to fit using Eq. (5) and theoretical $\lambda(T)$ assuming the BCS clean limit. From this fit, we obtain $\gamma\kappa/C = 88.56$, $\lambda_{ab}(0) = 1844$ Å, and $C\xi_c(0) = 20$ Å [$C\xi_c(T^*) = 102$ Å]. Also, the value of $\ln(\eta\alpha/\sqrt{e})$ is estimated to be 1.52 different from in the 2D system. Recalling that C is the order unity, we can conjecture that $\xi_c(0)$ is of order of $\sim$2 Å, which is comparable with $\xi_c(0)\sim$1.4 Å for

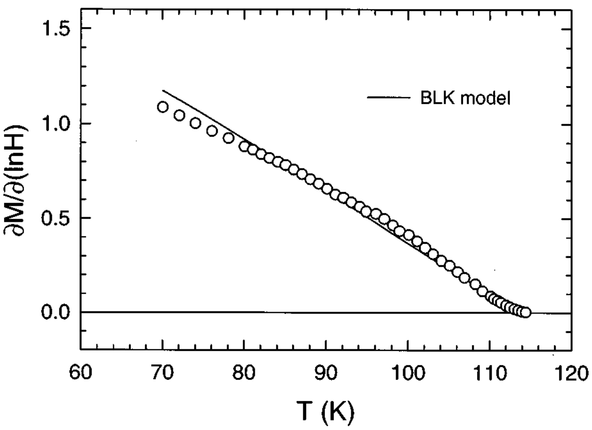

FIG. 4. Temperature dependence of the slope $\partial M/\partial \ln H$. Solid line represents theoretical fitting.

Y-123.[18] This large coherence length for out-of-plane means that the temperature range of 3D behavior (or critical region) is relatively wide, which can be also confirmed by high-field scaling analysis. According to Ullah *et al.*,[5] the magnetization in the critical region shows the scaling behavior as follows:

$$\frac{4\pi M}{(TH)^n}=F\left(A\frac{T-T_c(H)}{(TH)^n}\right), \tag{6}$$

where $F(x)$ is the scaling function but which is universal for all materials, A is a field and transition temperature independent coefficient, and n is 2/3 for a 3D system and 1/2 for a 2D system. Figure 5 shows the $4\pi M/(TH)^n$ versus the scaling parameter $(T-T_c(H))/(TH)^n$ with $n = 2/3$. For each field, all data is collapsed onto a single curve, consistent with Eq. (6). The slope $-dH_{c2}/dT = 1.95$ T/K near T_c is obtained from the above scaling analysis.

B. Temperature dependence of $\kappa(T)$

From reversible magnetization data, several important superconducting parameters can be extracted by applying the method developed by Hao *et al.* at temperatures where thermal fluctuations can be ignored. In this model, not only elec-

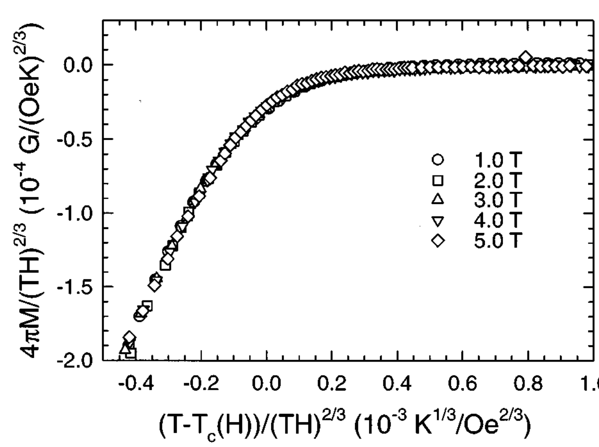

FIG. 5. Three-dimensional scaling of the magnetization in field range of between 1 T and 5 T.

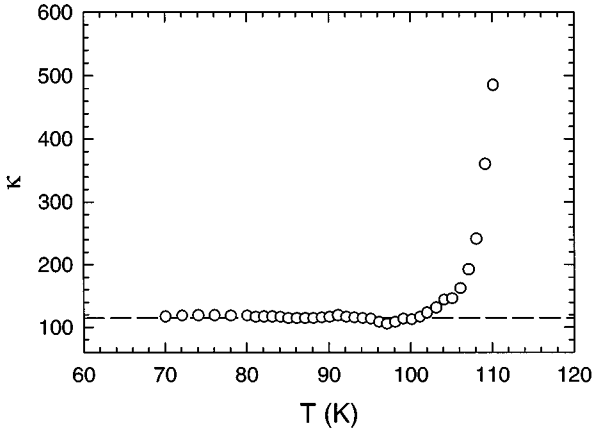

FIG. 6. Temperature dependence of Ginzburg-Landau parameter $\kappa(T)$ obtained from the theoretical fitting.

tromagnetic energy of vortex F_{em}, but also the core energy F_{core} is included in the total free energy. This is different from the London model. The contribution of F_{core} cannot be ignored for the magnetization at high fields.

Hao *et al.* assume, for the order parameter, a trial function as follows:

$$f=\frac{\rho}{(\rho^2+\xi_v^2)^{1/2}}f_\infty, \tag{7}$$

where ξ_v and f_∞ are variational parameters representing the effective core radius of a vortex and the depression in the order parameter due to overlapping of vortices, respectively. The reversible magnetization can be calculated from the Ginzburg-Landau free energy by using this trial function.

For the fitting of the magnetization data by using the model of Hao *et al.*, we choose a set of data $\{-4\pi M_i/f_v, H_i\}$ $(i=1,2,\ldots)$ at a fixed temperature in the temperature range 70 K$\leqslant T \leqslant$110 K. The details of the fitting procedure were described elsewhere.[7,19]

The $\kappa(T)$ extracted from the Hao-Clem procedure is shown in Fig. 6. In the temperature region of 70 K $\leqslant T\leqslant$ 100 K, the $\kappa(T)$ weakly increases with decreasing tempera-

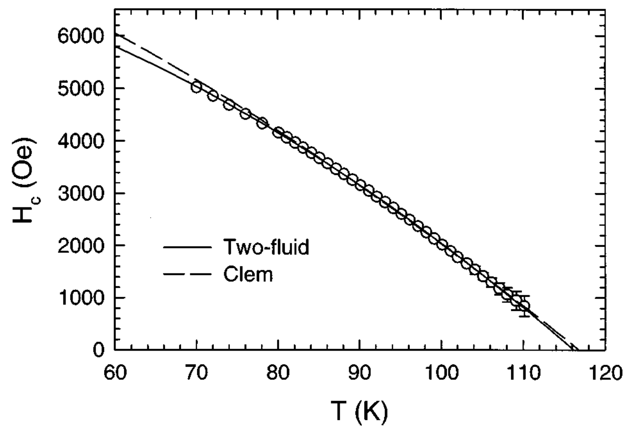

FIG. 8. Temperature dependence of thermodynamic critical field $H_c(T)$ obtained from the theoretical fitting. Solid and dashed lines represent the BCS temperature dependence of $H_c(T)$ and two fluid model, respectively.

ture. This behavior is typical for the Werthamer-Helfand-Hohenburg's theory.[20] It should be noted that the $\kappa(T)$ begins to increase abruptly for temperature near T = 100 K which is about $0.86T_c$. This anomalous behavior is due to the influence of positional fluctuation of vortices. But, unlike the Bi-2212, the temperature region of this anomalous behavior is significantly narrow, which may imply that vortex fluctuation effect is dominant in limited temperature regions near T_c. If the vortex fluctuation effect is more dominant for large anisotropic cases, the narrow region of anomalous behavior in the $\kappa(T)$ means that Hg-1212 is a moderately anisotropic superconductor such as Y-123 (Ref. 3) and Y-124 (Ref. 4). This is consistent with above vortex fluctuation and high field scaling analysis.

C. Theoretical representation of reversible magnetization with fixed κ

For the temperature region of 100 K$\leqslant T\leqslant T_c$, the extra free energy due to the distortion of vortices should be considered in describing the magnetization properly. However,

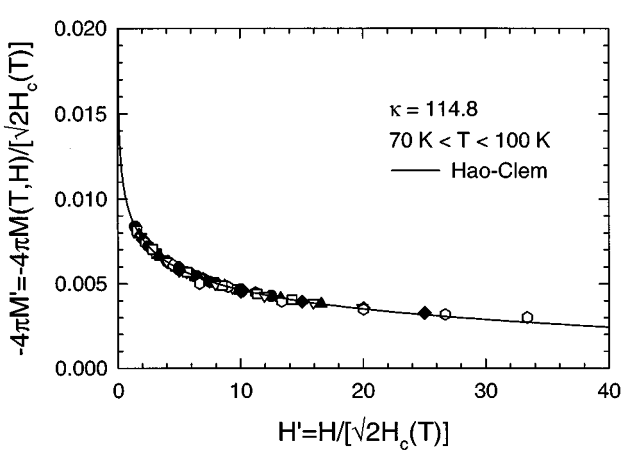

FIG. 7. The curves of $-4\pi M(H)$ scaled by $\sqrt{2}H_c(T)$. Solid line represents the universal curve of the model of Hao *et al.* with κ = 114.8.

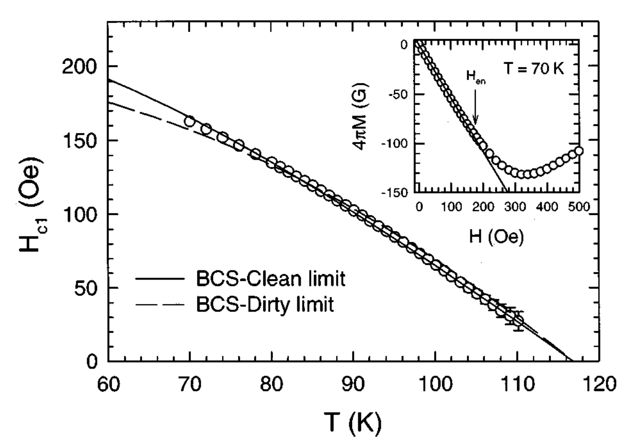

FIG. 9. Temperature dependence of lower critical field $H_{c1}(T)$ obtained from the theoretical fitting. Solid and dashed lines represent the BCS clean and dirty limits, respectively. Inset: external field dependence of magnetization $4\pi M(H)$ at T = 70 K.

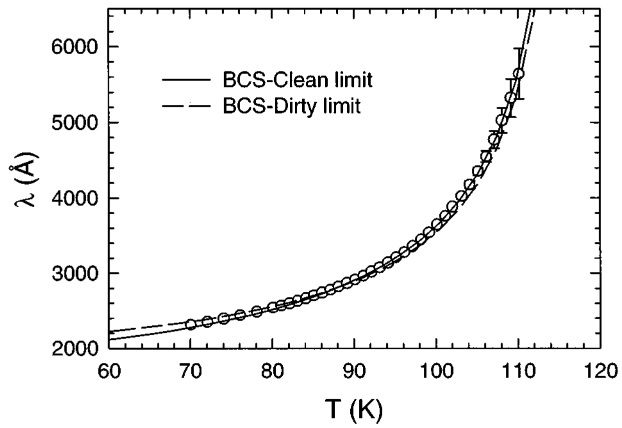

FIG. 10. Temperature dependence of penetration depth $\lambda(T)$ obtained from the theoretical fitting. Solid and dashed lines represent the BCS clean and dirty limits, respectively.

as mentioned above, the vortex fluctuation effect could be ignored comparing with F_{em} and F_{core} at the temperature range of 70 K $\leqslant T \leqslant$ 100 K. If we take the $\kappa_{av} = 114.8$ as the average value of $\kappa(T)$ in the limited temperature range of 70 K$\leqslant T \leqslant$100 K, then $-4\pi M(H)$ curves could be represented to an universal curve with scaling factor $\sqrt{2}H_c(T)$, consistent with the model of Hao *et al.* Figure 7 shows $-4\pi M' = -4\pi M/\sqrt{2}H_c(T)$ versus $H' = H/\sqrt{2}H_c(T)$ of experimental data and theoretical fitting. For each temperature, all data is collapsed onto a single curve.

From these results, the theoretical curves of $-4\pi M(T)$ are obtained using $-4\pi M(T) = -4\pi M'(H)\sqrt{2}H_c(T)$ at constant H. The solid line of Fig. 1 shows calculated $-4\pi M(T)$. Except for the dominant region of vortex fluctuation region, $M(T)$ is well described from the entire reversible temperature region by the model of Hao *et al.*

D. Critical fields and thermodynamic parameters

Figure 8 shows $H_c(T)$ vs T obtained from the above analysis. Near T_c, the error bar is somewhat large, because the vortex fluctuation effect is neglected. The solid and dashed lines represent the two-fluid model[21] and the BCS result,[22] respectively. These models yield $H_c(0) = 7911 \pm 10$ Oe and $T_c = 116.1 \pm 0.1$ K for the two-fluid model, while $H_c(0) = 8437 \pm 18$ Oe and $T_c = 116.8 \pm 0.1$ K for BCS model. According to the relation $H_{c2}(T) = \sqrt{2}\kappa H_c(T)$, the upper critical field slope, $(dH_{c2}/dT)_{T_c} = -2.01$ T/K, is estimated. This value is fairly consistent with the above scaling result. The slope can be used to estimate the upper critical field at $T = 0$ by using the formula[20]

$$H_{c2}(0) = 0.5758\left[\frac{\kappa_1(0)}{\kappa}\right]T_c\left|\frac{dH_{c2}}{dT}\right|_{T_c}. \tag{8}$$

In the dirty limit, $\kappa_1(0)/\kappa = 1.20$, while in the clean limit, $\kappa_1(0)/\kappa = 1.26$.[20] From this formula, $H_{c2}(0)$ is estimated 170.4 T [$\xi_{ab}(0) = 13.9$ Å] assuming the clean limit, and 162.3 T ($\xi_{ab}(0) = 14.2$ Å) assuming the dirty limit.

The lower critical field $H_{c1}(T)$ could be obtained from the model of Hao *et al.*

$$H_{c1}(T) = \sqrt{2}H_c(T)\left(\frac{\kappa\xi_{v0}^2}{8} + \frac{1}{8\kappa} + \frac{K_0(\xi_{v0})}{2\kappa\xi_{v0}K_1(\xi_{v0})}\right), \tag{9}$$

where $K_n(x)$ is a modified Bessel function of nth order. Figure 9 shows the temperature dependence of $H_{c1}(T)$. The

TABLE I. Thermodynamic parameters of $HgBa_2Ca_{0.86}Sr_{0.14}Cu_2O_{6-\delta}$, $YBa_2Cu_3O_{7-\delta}$, and $Bi_2Sr_2CaCu_2O_{8-\delta}$.

	Hg-1212	Y-123	Bi-2212
κ	114.8	57 ± 5 (Ref. 7)	< 185 ± 11 (Ref. 23)
		72 (Ref. 24)	
$-dH_{c2}/dT\|_{T_c}$ (T/K)	2.01	1.65 ± 0.23 (Ref. 7)	2.5 ± 0.2 (Ref. 23)
	1.95 (scaling)	1.9 (Ref. 3)	
$H_{c2}(0)$ (T)	170.4[a]	112 (Ref. 7)	158 ± 13 (Ref. 23)
	162.3[b]		86 (Ref. 25)
$H_{c1}(0)$ (Oe)	234[a]		
	199[b]		
$H_c(0)$ (Oe)	8437 ± 18	1.10×10^4 (Ref. 7)	
		1.18×10^4 (Ref. 24)	
$\lambda_{ab}(0)$ (Å)	1913[a]	1310 ± 30 (Ref. 24)	< 2630 ± 160 (Ref. 23)
	2130[b]		
	1844 (BLK)		
$\xi_{ab}(0)$ (Å)	13.9[a]	17.2 ± 1.2 (Ref. 7)	20.4 (Ref. 26)
	14.2[b]	18.1 ± 1 (Ref. 24)	21.4 (Ref. 25)
		13.6 ± 0.8 (Ref. 18)	0.37 (Ref. 26)
$\xi_c(0)$ (Å)	> 2 (BLK)	1.23 ± 0.19 (Ref. 18)	0.4 (Ref. 25)
γ	< 7.7 (BLK)	≃ 5 (Ref. 27)	≃ 55 (Ref. 28)
$\ln(\eta\alpha/\sqrt{e})$	1.52 (BLK)		1 (Ref. 14)

[a]BCS clean limit.
[b]BCS dirty limit.

solid and dashed lines represent the BCS clean and dirty limits, respectively. In the clean limit, $H_{c1}(0)$ is 234 Oe, while in the dirty limit, $H_{c1}(0)$ is 199 Oe. More specifically, the computed H_{c1} at $T = 70$ K is 163 Oe. This value is consistent with the flux entry field $H_{\mathrm{en}}(\geqslant H_{c1}) \simeq 170$ Oe which is estimated from the $M(H)$ curve as shown in the inset of Fig. 9.

The penetration depth $\lambda(T)$ is evaluated by using the relation $\lambda = \kappa(\phi_0/2\pi H_{c2})^{1/2}$ as shown in Fig. 10. The solid and dashed lines show the best fit of BCS clean and dirty limits, respectively. The data fits the clean limit better than the dirty limit. From the fitting results, $\lambda_{ab}(0)$ is estimated to be 1913 Å assuming the clean limit, and 2130 Å assuming the dirty limit. The value for clean limit is consistent with that from vortex fluctuation analysis. These results are summarized in Table I with parameters of Y-123 and Bi-2212 for the comparison. The total errors of our superconducting parameters from all sources including the sample quality and the experimental errors are estimated to be less than 20%.

IV. CONCLUSIONS

The reversible magnetization for grain-aligned $HgBa_2Ca_{0.86}Sr_{0.14}Cu_2O_{6-\delta}$ was measured with magnetic fields parallel to the c axis. Clear evidence of vortex fluctuation was observed, i.e., a field independent magnetization. From the BLK model and the model of Hao *et al.*, $\gamma\kappa/C = 88.6$ and $\kappa = 114.8$ were obtained. The upper limit of the anisotropy ratio was estimated to be 7.7, which means that Hg-1212 can be described by Ginzburg-Landau functional with anisotropic masses. The confident evidence supporting to be 3D system can be found from that the high-field magnetization at critical region follows 3D scaling law. In the temperature range of 70 K$\leqslant T \leqslant$100 K, the reversible magnetization is well described by variational approaches of Hao *et al.* From the fits of the model of Hao *et al.*, we obtained various superconducting parameters. These derived values are consistent with those from 3D high-field scaling results and 3D vortex fluctuation analysis.

ACKNOWLEDGMENTS

We wish to express appreciation for the financial support of the Korean Ministry of Education, Basic Science Research Centers of Pohang University of Science and Technology, Agency of Defense Development of Korea, and Korea Science and Engineering Foundation.

[1] L. N. Bulaevskii, M. Ledvij, and V. G. Kogan, Phys. Rev. Lett. **68**, 3733 (1992).
[2] V. G. Kogan *et al.*, Phys. Rev. Lett. **70**, 1870 (1993).
[3] U. Welp *et al.*, Phys. Rev. Lett. **67**, 3180 (1991).
[4] J. Sok *et al.*, Phys. Rev. B **51**, 6035 (1995).
[5] S. Ullah and A. T. Dorsey, Phys. Rev. Lett. **65**, 2066 (1990).
[6] Z. Hao and J. R. Clem, Phys. Rev. Lett. **67**, 2371 (1991).
[7] Z. Hao *et al.*, Phys. Rev. B **43**, 2884 (1991).
[8] N. H. Hur *et al.*, Physica C **231**, 227 (1994).
[9] N. H. Hur *et al.*, Physica C **231**, 4 (1994).
[10] P. G. Radaeli *et al.*, Physica C **216**, 29 (1993).
[11] D. E. Farrell *et al.*, Phys. Rev. B **36**, 4025 (1987).
[12] A. A. Abrikosov, Zh. Éksp. Teor. Fiz. **32**, 1442 (1957).
[13] M. Tinkham, *Introduction to Superconductivity* (McGraw-Hill, New York, 1980).
[14] Z. Tešanović and A. V. Andreev, Phys. Rev. B **49**, 4064 (1994).
[15] Z. Tešanović *et al.*, Phys. Rev. Lett. **69**, 3563 (1992).
[16] Q. Li, M. Suenaga, T. Hikata, and K. Sato, Phys. Rev. B **46**, 5857 (1992).
[17] L. Fabregá *et al.*, Europhys. Lett. **24**, 595 (1993).
[18] W. C. Lee, R. A. Klemm, and D. C. Johnston, Phys. Rev. Lett. **63**, 1012 (1989).
[19] M.-S. Kim, M.-K. Bae, W. C. Lee, and S.-I. Lee, Phys. Rev. B **51**, 3261 (1995).
[20] N. R. Werthamer, E. Helfand, and P. C. Hohenberg, Phys. Rev. **147**, 295 (1966).
[21] C. J. Gorter and H. B. G. Casimir, Physica **1**, 306 (1934).
[22] J. R. Clem, Ann. Phys. (N.Y.) **40**, 286 (1966).
[23] H.-C. Ri *et al.*, Phys. Rev. B **50**, 3312 (1994).
[24] J. Gohng and D. K. Finnemore, Phys. Rev. B **46**, 398 (1992).
[25] R. Jin, A. Schilling, and H. R. Ott, Phys. Rev. B **49**, 9218 (1994).
[26] W. C. Lee, J. H. Cho, and D. C. Johnston, Phys. Rev. B **43**, 457 (1991).
[27] D. R. Harshman *et al.*, Phys. Rev. B **39**, 851 (1989).
[28] M. J. Naughton *et al.*, Phys. Rev. B **38**, 9280 (1988).